

Deformational response of a marine silty-clay with varying organic content in the triaxial compression space

Ponzoni, Elisa; Muraro, Stefano; Nocilla, Alessandra; Jommi, Cristina

DOI

[10.1139/cgj-2023-0058](https://doi.org/10.1139/cgj-2023-0058)

Publication date

2023

Document Version

Final published version

Published in

Canadian Geotechnical Journal

Citation (APA)

Ponzoni, E., Muraro, S., Nocilla, A., & Jommi, C. (2023). Deformational response of a marine silty-clay with varying organic content in the triaxial compression space. *Canadian Geotechnical Journal*, 61 (2024)(9), 1819-1831. <https://doi.org/10.1139/cgj-2023-0058>

Important note

To cite this publication, please use the final published version (if applicable).
Please check the document version above.

Copyright

Other than for strictly personal use, it is not permitted to download, forward or distribute the text or part of it, without the consent of the author(s) and/or copyright holder(s), unless the work is under an open content license such as Creative Commons.

Takedown policy

Please contact us and provide details if you believe this document breaches copyrights.
We will remove access to the work immediately and investigate your claim.

Green Open Access added to TU Delft Institutional Repository

'You share, we take care!' - Taverne project

<https://www.openaccess.nl/en/you-share-we-take-care>

Otherwise as indicated in the copyright section: the publisher is the copyright holder of this work and the author uses the Dutch legislation to make this work public.

Deformational response of a marine silty-clay with varying organic content in the triaxial compression space

Elisa Ponzoni^a, Stefano Muraro^b, Alessandra Nocilla^c, and Cristina Jommi^{b,d}

^aRina S.p.A., Via Antonio Cecchi, 6, 16129 Genova, Italy; ^bDepartment of Geoscience and Engineering, Delft University of Technology, Delft, 2628 CN, The Netherlands; ^cDepartment of Civil Engineering, Architecture, Land and Environment, and Mathematics, Università di Brescia, Brescia, 25123, Italy; ^dDepartment of Civil and Environmental Engineering, Politecnico di Milano, piazza Leonardo da Vinci 32, 20133, Milano, Italy

Corresponding author: **Stefano Muraro** (email: S.Muraro@tudelft.nl)

Abstract

This study characterises the effects of naturally varying organic content on the compression and shear behaviour of a marine silty-clay from the Netherlands. Index properties and mechanical properties are determined through laboratory tests, including oedometer and multistage loading-unloading triaxial stress paths. The results indicate a significant impact of the organic content on the compression response, with both the loading and reloading indexes increasing as the loss on ignition increases from 3% to 7%. Additionally, the study suggests a directional response of the compression behaviour, with the loading index increasing with the stress ratio. The influence of the organic content on shear strength appears to be less significant. No brittle response is observed during shearing, and a similar ultimate stress ratio is attained by all samples. However, a unique critical state line can only be identified for samples with similar organic content, as its intercept and slope are found to increase with increasing organic content. The experimental results from stress paths at constant stress ratio reveal an anisotropic pre-failure plastic deformation mode, which depends on the previous stress history and loading direction. This suggests that the stress–dilatancy relationship cannot be formulated as a unique function of the stress ratio. The high-quality experimental data presented in the study enlarge the database on soft organic soils in view of the development of advanced constitutive models.

Key words: soft soils, triaxial tests, compression behaviour, shear behaviour, organic matter

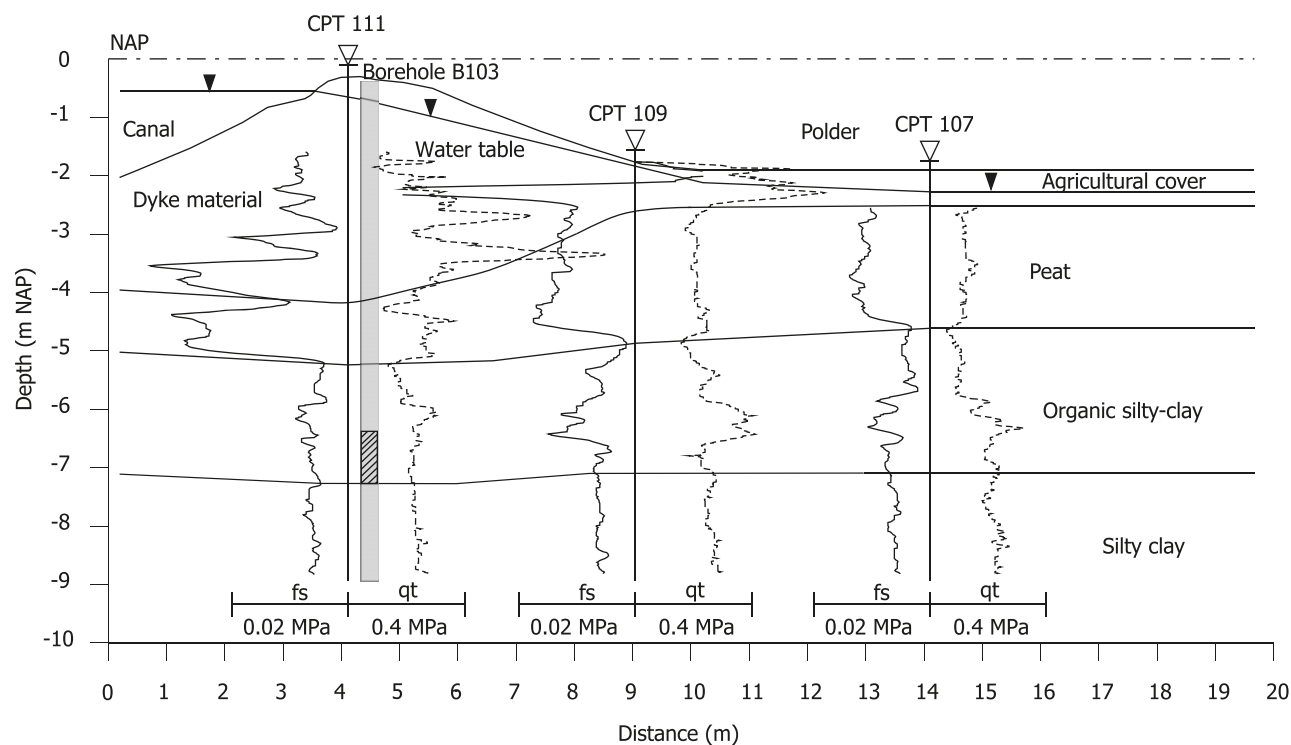
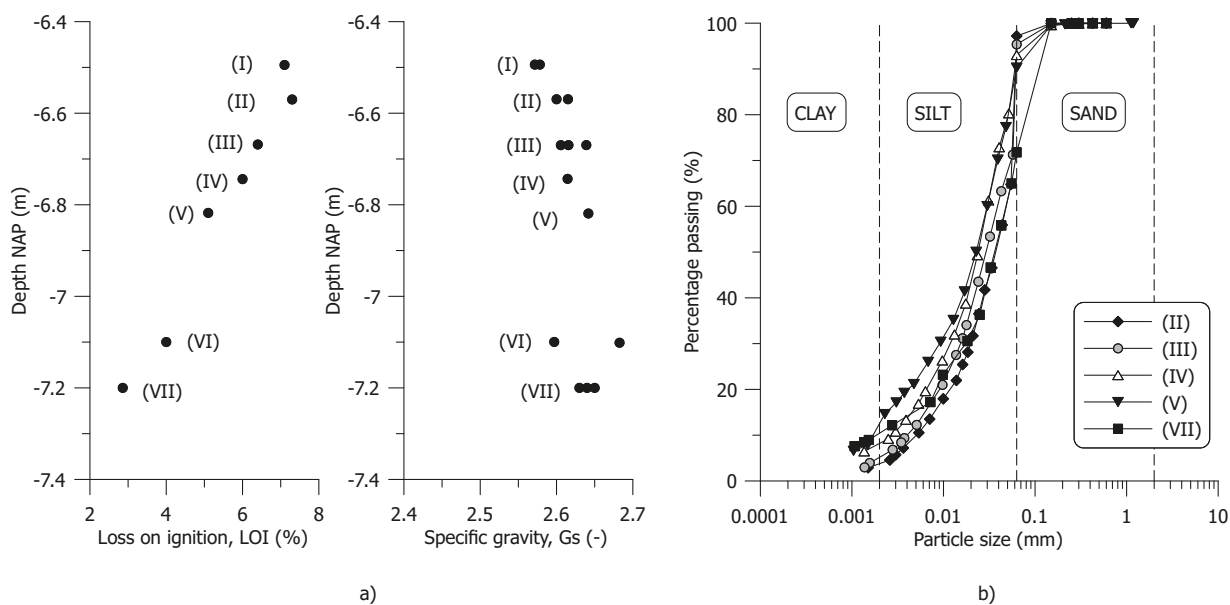
Introduction

In the Netherlands, soft soils represent a large portion of natural geo-materials within the sub-surface and serve as foundation layers for a vast range of structures and infrastructures. The advanced characterisation of the geotechnical behaviour of soft soils is essential to support the development of constitutive models used more and more frequently in the assessment and design practice.

In the past, extensive research focused on investigating the geotechnical behaviour of peat, which is traditionally considered the critical soil foundation layer for the stability of earth structures. Field tests on existing and trial embankments and extensive experimental laboratory tests have been performed on peat in the last decades (Den Haan and Kruse 2007; Zwanenburg et al. 2012; Zwanenburg and Jardine 2015; Muraro and Jommi 2021). A recent field test on a regional dyke at the Leendert de Boerspolder near Leiden shed light on the behaviour of the different soft soil foundation layers in the pre-failure and failure mechanism (Muraro 2019; Jommi et al. 2021). Contrary to the common assumption of peat being the weak soil layer, the field test showed that the stiffer organic silty-clay underlying the foundation peat was the critical layer where failure was triggered. The interface between

peat and silty-clay had also been identified as the weak soil surface by Hendry et al. (2013) in the analysis of the stability of railway embankments founded on peat. Despite the large body of experimental research on peat, to the authors' knowledge, a systematic characterisation of the geotechnical behaviour of Dutch organic clays is still lagging behind except for the Oostvaardersplassen clay (Tigchelaar et al. 2001; Den Haan 2003; Cheng et al. 2007).

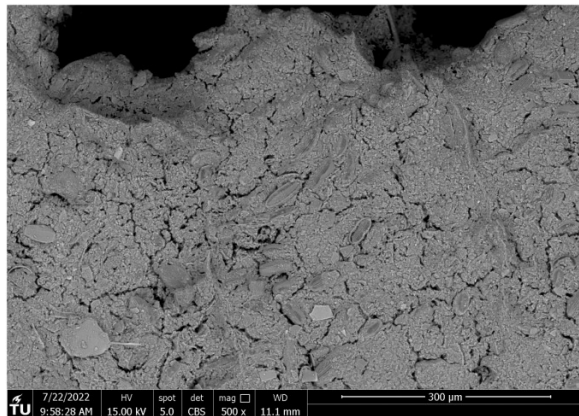
The geotechnical behaviour of these soils appears to be strongly influenced by the peculiar characteristic of their fabric, which often contains amorphous organic matter, fibres, stems, wood fragments, and microorganisms such as algae and plankton, together with silicate and calcium microfossils (e.g., Cheng et al. 2004; Cheng et al. 2007). The extensive research conducted to characterise the compression and shear behaviour of similar soils from all over the world brought to a broad distinction between diatomaceous (e.g., Ariake clay, Hachirogata clay, Osaka Bay clay, Mexico City clay, and Bogotá clay) and non-diatomaceous or slightly diatomaceous soft soils (e.g., Bothkennar clay, Pusan clay, Bangkok clay, Singapore clay, and Oostvaardersplassen clay). The presence of diatom microfossils has been found to have a remarkable impact on the engineering behaviour of such soils. Due to their

Fig. 1. Cross-section stratigraphy profile of the test site at the Leendert de Boerspolder.**Fig. 2.** (a) Profile of loss on ignition and specific gravity and (b) particle size distributions of the tested material.

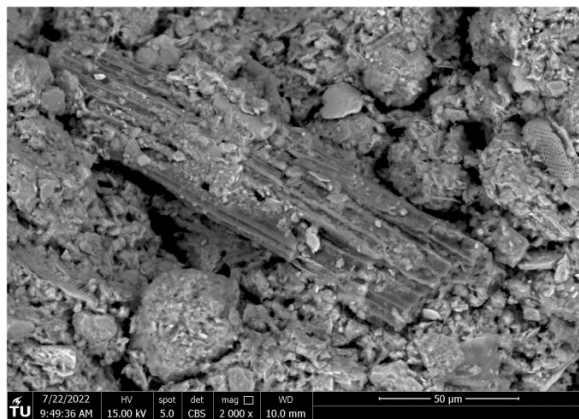
hollow skeleton and the entrapped water in their intraskeletal pore space, diatoms increase the Atterberg's limits and plasticity, void ratio, hydraulic conductivity, and compressibility (Lo 1962; Mesri et al. 1975; Diaz-Rodriguez et al. 1992; Tanaka and Locat 1999; Caicedo et al. 2018). Besides the increase in soil compressibility, diatomaceous soils exhibit exceptionally high friction angles due to the rough surface and interlocking of diatoms with the soil fabric (Shiwakoti et al. 2002).

For non-diatomaceous soils, the organic matter in the form of microorganisms, fibres, stems, leaves, and amorphous matter predominates in the engineering response. Residues of marine organisms (e.g., planktonic and benthic), such as in the soil matrix of Bothkennar clay, were found to have important effects on the soil plasticity and compressibility due to organic cement contributing to sustaining large soil aggregates or pellets (Hight et al. 1992; Paul and Barras 1999). However, following Hight et al. (1992), this microorganism-related

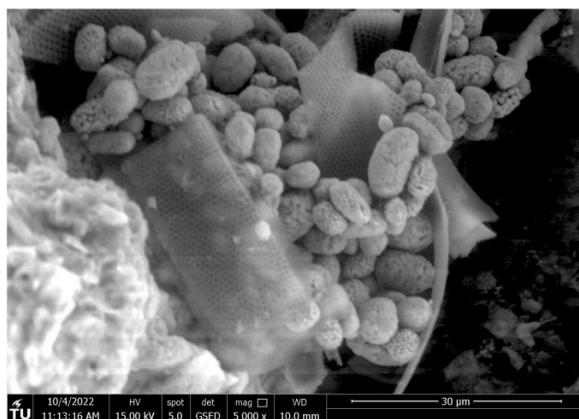
Fig. 3. Environmental scanning electron microscope (ESEM) photomicrographs taken on independent soil samples at different magnification levels: (a) 500 \times (LOI = 4%), (b) 2000 \times (LOI = 4%), and (c) 5000 \times (LOI = 3%).



a)



b)



c)

organic matter is unlikely to affect the shearing resistance. On the contrary, the organic material of terrestrial plant origin significantly alters the shear strength of soil through reinforcing effects. The abundance of micro-fibres in the soil matrix increases the soil friction angle significantly. Friction angles even above 60° were reported by Larsson (1990) for

Swedish organic clay and gyttja with micro-fibres in the soil matrix.

In the Netherlands, silty-clays are found including both diatoms and fibres from plant origin. Extensive characterisation can be found in the literature for the Oostvaarder-splassen clay, where wood fragments, stems, rootlets, and micro-fibres co-exist with microorganisms such as algae and plankton, amorphous organics and silicate, and calcium carbonate microfossils (Tigchelaar et al. 2001; Den Haan 2003). This study presents a systematic characterisation of an organic silty-clay found in the foundation of the full-scale test at Leendert de Boerspolder (Jommi et al. 2021). The soil is found in a marine prevalently silty parent area formed during the Holocene (de Bakker 1979). Oedometer and multistage triaxial stress paths are conducted on undisturbed samples with varying organic content and diatomaceous inclusions. The pre-failure compression and shear response and strength are evaluated. The experimental data presented in this study improve existing datasets for the development of constitutive models for soft organic soils relevant to the engineering practice.

Experimental programme

Material and soil characterisation

The soil used in this study was retrieved at the Leendert de Boerspolder site in the Netherlands. The soil profile is reported in Fig. 1 and consists of (a) heterogeneous dyke material (i.e., silty sand with traces of gravel and clay, clayey silt with traces of sand), (b) peat layer with a thickness between 1 m below the crest of the dyke and 2.5 m at the polder side, (c) organic silty-clay deposit ~2 m thick characterised by variable organic content, (d) thick deep silty-clay layer, and (e) deep Pleistocene sand layer (not displayed in Fig. 1). The Normaal Amsterdam Peil, NAP, is used as a reference system for elevation. The water level in the canal and the polder was regulated by the managing waterboard with small variations over time. The phreatic surface was located 0.3 m below the crest of the dyke at -0.6 m NAP. The dyke material was slightly overconsolidated (maximum overconsolidation ratio OCR equal to 2.0) in the upper part, while the OCR decreased with depth towards the normally consolidated state at the interface with the peat layer. The underlying peat layer and organic silty-clay were slightly overconsolidated or normally consolidated (Ponzoni 2017).

The experimental data presented in the following refer to the organic silty-clay soil layer. The samples were retrieved between -6.5 and -7.2 m NAP below the crest of the dyke using a 106 mm diameter piston sampler.

To reduce bio-degradation, the material was stored in a climate-controlled room at 10 ± 1 °C and 90% relative humidity. To avoid loss of organic matter, oven-drying procedures for soil classification were performed at a temperature of 60 °C (Head 2014). The specific gravity of the soil, G_s , was measured with a helium pycnometer (D5550-14 2014). The loss on ignition, LOI, was determined by igniting oven-dried samples in a furnace at 440 °C (D2974-14 2014). The loss on ignition is used as a proxy of the variable organic content

Table 1. Index properties, initial state, and stress path of the tested specimens.

Tube	Sample ID	Test	LOI (%)	Group	e_i (-)	p'_c (kPa)	p'_s (kPa)
B103-13	T1	Oedometer	7.1	I	2.13	–	–
	T2	Oedometer	7.1		2.30	–	–
B103-13	T1	TxCU*	7.3	II	2.03	13	13
	T2	TxCU	7.3		2.00	25	25
	T3	TxCU	7.3		2.07	47	47
B103-13	T1	Isotropic	6.4	III	1.93	149	26
	T2	K_0 ***	6.4		1.93	–	11
	T3	Mixed****	6.4		1.82	67	36
B103-13	T1	Mixed	6.0	IV	1.78	64	36
	T2	Mixed	6.0		1.63	68	36
	T3	TxCU	6.0		1.79	80	80
B103-13	T1	Oedometer	5.1	V	1.55	–	–
	T2	Oedometer	5.7		1.86	–	–
B103-14	T1	p' constant	4.0	VI	1.27	14	14
	T2	TxCD**	4.0		1.31	14	14
B103-14	T1	Isotropic	2.9	VII	1.50	120	120
	T2	K_0	2.9		1.42	–	7

*Undrained triaxial compression test. **Drained triaxial compression test. *** K_0 triaxial compression at null lateral strain. ****Mixed: Various combinations of stress paths at constant stress ratio, p' constant loading unloading and q constant paths (see Fig. 4 for the specific soil samples).

over depth. The tested material was divided into seven groups based on the loss on ignition as shown in Fig. 2a. The decrease of the LOI over depth from 7.3%–2.9% is reflected in a general increase in the specific gravity. Figure 2b reports the particle size distribution from wet-sieving and hydrometer analysis for some of the tested groups (BS1377 1996; Head 2014). The soil composition ranges from silt with traces of sand and clay to clayey sandy silt. The comparison in Fig. 2 suggests that the organic matter is mainly included in the silty fraction. The plastic and liquid limits range from $w_p = 0.261$ to 0.408 and from $w_l = 0.369$ to 0.774 with an LOI of 2.7% and 6.4%, respectively.

An impression of the fabric of the tested material is displayed in Fig. 3 from three independent environmental scanning electron microscope (ESEM) photomicrographs taken on natural samples with LOI = 3%–4%. The fabric is organised in aggregates with a characteristic size of 50–100 μm where silty particles, diatoms inclusions (Fig. 3a), small wood fragments (Fig. 3b), and pyrite framboids (Fig. 3c) are visible.

Relevant index properties of the samples are reported in Table 1, together with the initial void ratio of the natural samples, e_i ; the pre-consolidation mean effective stress applied in each test, p'_c ; the mean effective stress at the start of the shear, p'_s ; and an indication of the stress path followed during each test. All the samples were tested in undisturbed conditions except for one reconstituted sample, T2 (V), prepared with a water content equal to the limit liquid (Burland 1990).

The nominal size of the tested specimens was 65 mm in diameter and 22 mm in height for incremental loading oedometer tests and 38 mm in diameter and 76 mm in height for triaxial tests. The triaxial system includes a submersible 1 kN load cell, a back pressure and cell pressure-

volume controllers with an accuracy of ± 1 kPa on pressure, and ± 300 mm³ on volume (0.15% full-scale range). A suction cap was used to ensure perfect contact between the load cell and the top cap given the low effective confining stresses adopted in the experimental investigation. All the drained tests were performed under stress control assuring that the maximum excess pore pressure remained below 5% of the mean effective stress imposed on the samples.

Stress and strain variables

The experimental data from triaxial tests are elaborated by assuming axisymmetric test conditions and adopting the common triaxial stress-strain variables: mean effective stress, p' ; deviatoric stress, q ; volumetric strain, ε_p ; and deviatoric strain, ε_q . Natural strains (Ludwik 1909) are adopted to elaborate the experimental data to avoid bias in the data interpretation due to the large displacements attained by the samples (Jommi et al. 2021):

$$(1) \quad \varepsilon_p = \varepsilon_a + 2\varepsilon_r = \ln\left(\frac{V_0}{V}\right)$$

$$(2) \quad \varepsilon_q = \varepsilon_a - \frac{\varepsilon_p}{3} = \ln\left(\frac{H_0}{H}\right) - \frac{1}{3}\ln\left(\frac{V_0}{V}\right)$$

where V_0 and H_0 are the initial volume and height of the sample, respectively, V and H are the correspondent current values during the test, ε_a is the axial strain, and ε_r is the radial strain. Compressive stresses and strains are assumed positive.

Stress paths

To investigate the volumetric behaviour, oedometer tests and isotropic and K_0 compression tests were performed. The K_0 compression tests were carried out in the triaxial apparatus with a radial stress ramp. Volume change and axial

Fig. 4. Experimental stress paths followed in the triaxial tests for groups of samples with different loss on ignition: (a) group (II), (b) groups (VI) and (VII), (c) group (IV), and (d and e) group (III).

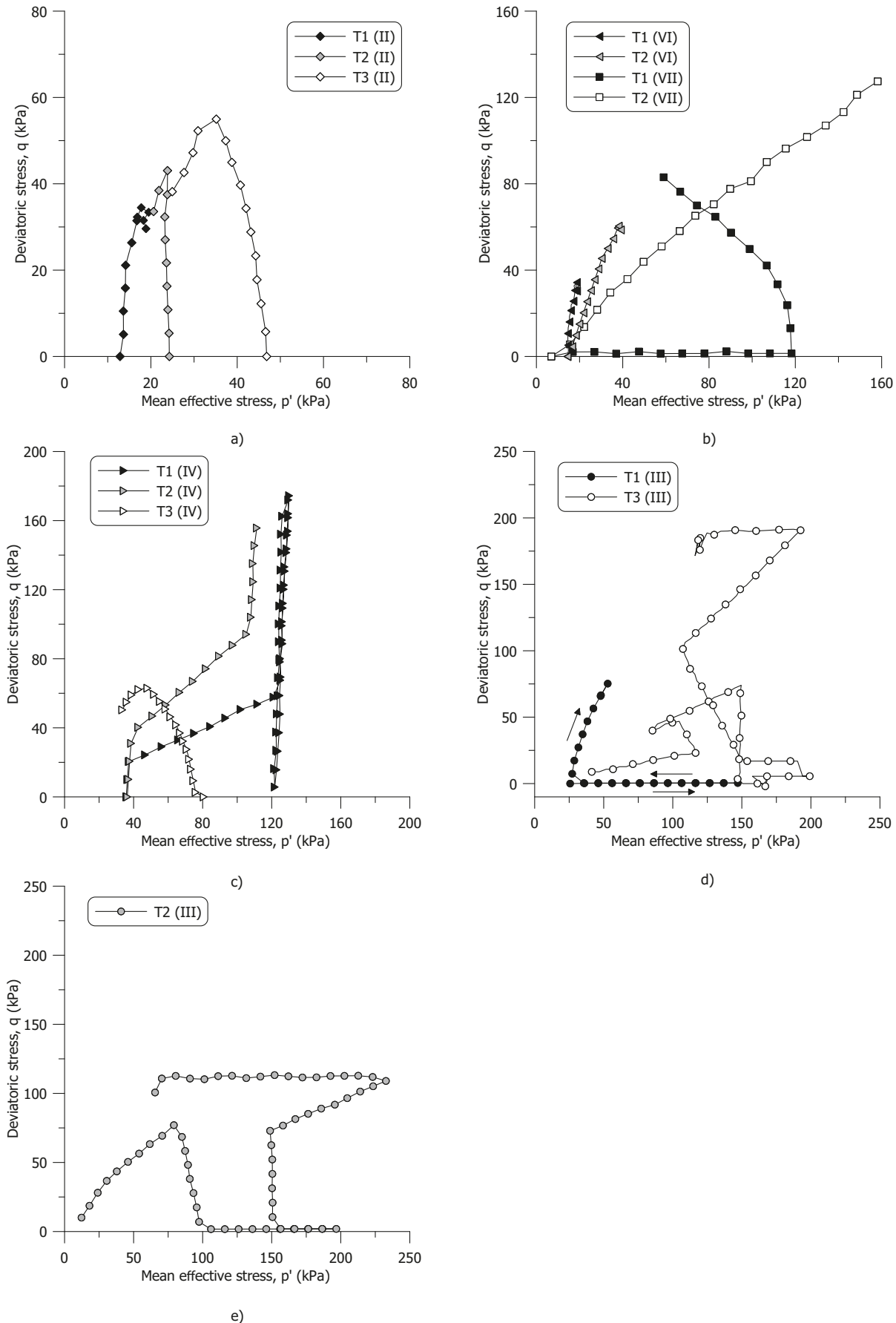
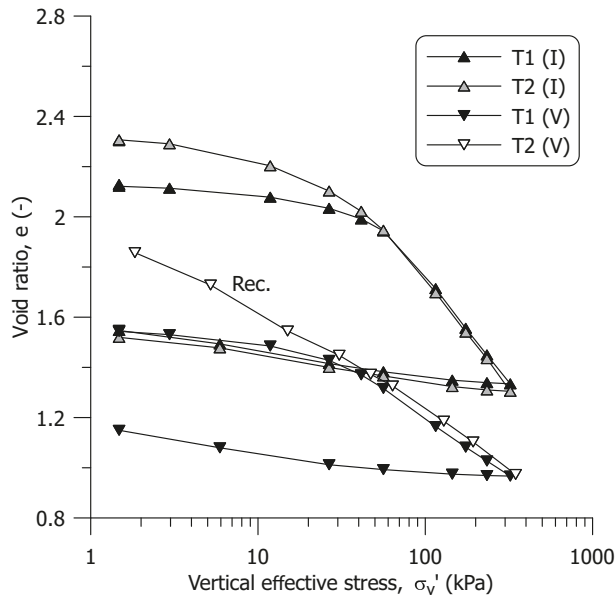


Fig. 5. Oedometer curves for samples from groups (I) and (V).



displacement back measurements allowed for automatic adjustment to guarantee negligible radial strains. Few samples were consolidated isotropically to p'_c to detect the initial yield surface. Afterwards, they were unloaded back to the isotropic stress p'_s indicated in Table 1. Eventually, the samples were sheared following different constraints (Fig. 4). Samples from group (II) were brought to failure with standard TxCU tests (Fig. 4a). Groups (VI) and (VII) were sheared following standard TxCU, TxCD, and approximately constant p' after isotropic compression (Fig. 4b). Multistage loading-unloading, compression at constant stress ratio, constant p' , and constant q stress paths were followed on the samples of groups (III) and (IV) to better evaluate the non-monotonic pre-failure response (Figs. 4c, 4d, and 4e).

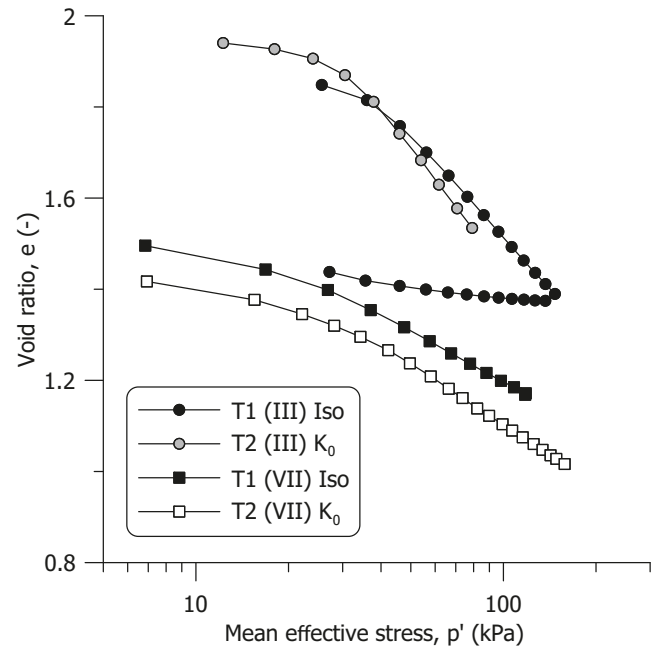
Experimental results

Compression behaviour

The oedometer tests performed on samples T1 (I), T2 (I), and T1 (V) allow identifying the effects of the organic matter on the compression behaviour as presented in Fig. 5. A unique one-dimensional compression line, 1D-VCL, can be identified for each tested group. For group (I) with a LOI equal to 7.1%, the 1D-VCL has a slope C_c equal to 0.83 ($\lambda \cong C_c/2.3 = 0.36$), whereas the inclination C_s of the unloading-reloading line (URL) has a value of 0.092 ($\kappa \cong C_s/2.3 = 0.04$). For group (V) with a LOI of 5.1%, $C_c = 0.46$ ($\lambda = 0.20$) and $C_s = 0.05$ ($\kappa = 0.022$) are found. The comparison between the natural T1 sample and reconstituted T2 sample from group (V) seems to suggest no significant destructuration effects for the tested material within the investigated stress range.

The response upon isotropic and K_0 compression in the tri-axial tests on samples from group (III), LOI of 6.4%, and group (VII) with the lowest LOI of 2.9% is shown in Fig. 6. The slope

Fig. 6. Isotropic and K_0 compression data for samples from groups (III) and (VII).



of the ISO-NCL line decreases with the LOI from 0.32 to 0.16 and the slope of the K_0 compression test (1D-VCL) from 0.36 to 0.19. The slope of the unloading-reloading line from sample T1 (III) has a value of 0.036.

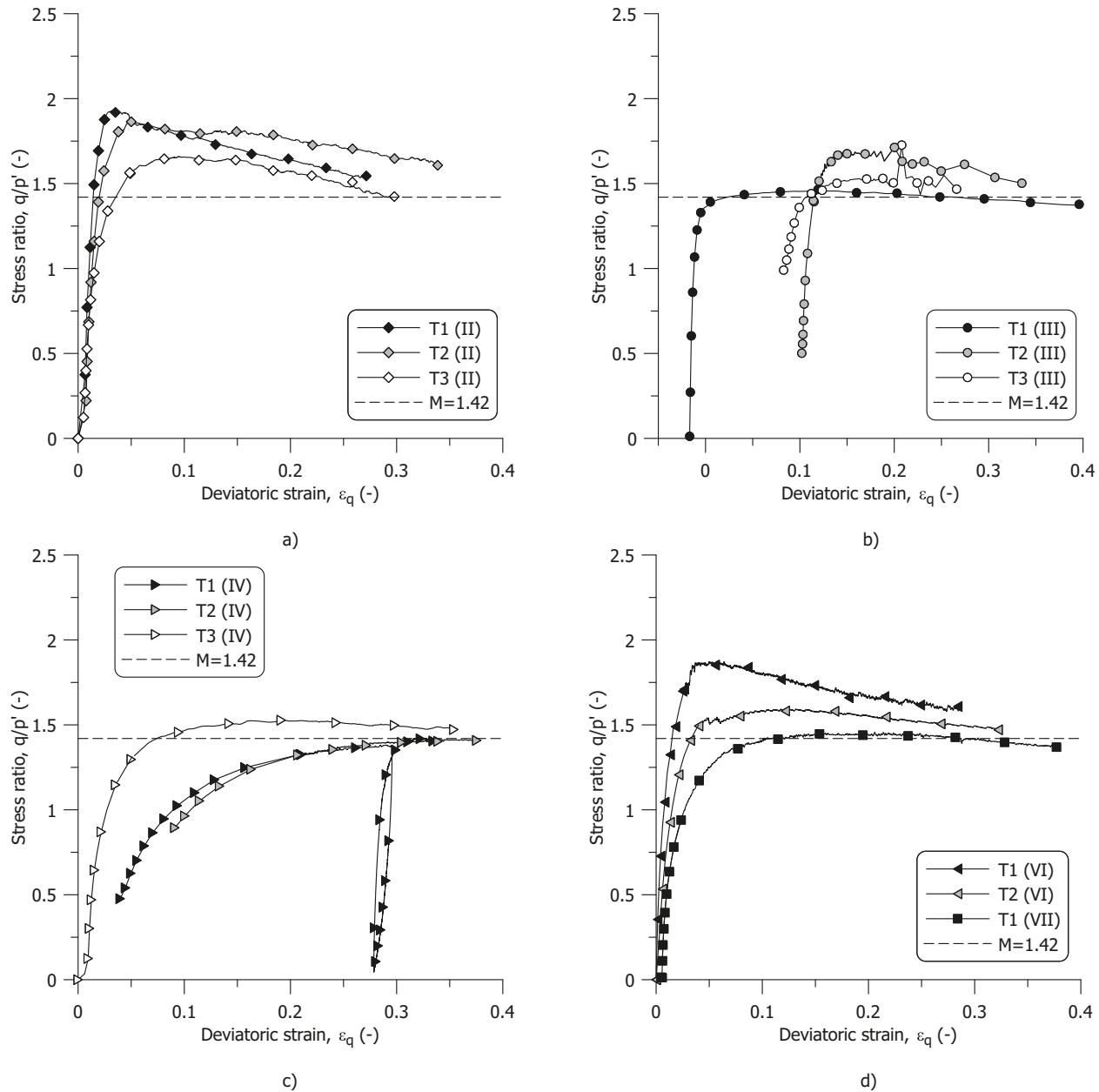
Shear behaviour

The sample response upon shearing is summarised in Fig. 7 in terms of stress ratio, q/p' , versus deviatoric strain for different groups of samples. For the sake of clarity, only the last portion of the stress path bringing each sample to failure is plotted.

The results in Fig. 7 suggest that the influence of the organic matter on the shear behaviour is less relevant compared to what was observed in the compression response. An ultimate stress ratio, M , equal to 1.42 ($\phi' = 35^\circ$) can be identified for almost all the sample groups. Only the samples from groups (II) and (VI) tested at very low confining stresses, $p' < 25$ kPa, attain a higher peak stress ratio equal to 1.8, followed by an asymptotic decrease towards the ultimate stress ratio of 1.42. Small fluctuations in the peak stress ratio are also found for samples T2 (III) and T3 (III) tested in stress-controlled unloading at constant deviatoric stress, which results in poor controllability when the samples approach failure (Fig. 4b). No significant brittle response is observed upon shearing except for the overconsolidated samples T1 (II) and T2 (II), which seems to confirm the absence of any significant destructuration for the tested material, as already anticipated from the compression behaviour.

The ultimate friction angle $\phi' = 35^\circ$ gives a consistent estimate of the at-rest lateral earth pressure coefficient in normally consolidated conditions using Jaky's simplified relationship ($K_0 \cong 1 - \sin \phi' = 0.426$) compared to the experimen-

Fig. 7. Stress ratio versus deviatoric strain during the final shearing stage up to failure for groups of samples with a different loss on ignition: (a) group (II), (b) group (III), (c) group (IV), and (d) groups (VI) and (VII).



tal value, $K_0 = 0.425$, determined from sample T2 (III) (Fig. 8). The value of K_0 at normally consolidated state for the tested material agrees well with literature data on various marine clays with similar plasticity index ($0.20 < I_p < 0.40$) (Watabe et al. 2003).

The ultimate state attained by the different samples is presented in the $e-p'$ space in Fig. 9. The data suggest that it is possible to identify a critical state line for samples belonging to the same group within the investigated stress level. The position of the critical state line (i.e., intercept, Γ) and slope (λ) are ruled by the loss on ignition. As indicated in Fig. 9, a general trend is observed with Γ and λ increasing with LOI with the exception of the two samples from group (VI).

Discussion

Effects of organic matter and loading direction on the compression behaviour

A comprehensive summary of the slope of the compression line and unloading-reloading line for samples with different LOI is presented in Fig. 10 based on the different stress paths in Fig. 4.

The results confirm the significant role of the organic matter on the compression behaviour of the tested material. The slope of the compression line decreases from 0.360 to 0.160 for an LOI of 7.1% and 2.9%, respectively. The effect is also visible on the unloading-reloading line with a slope decreasing

Fig. 8. Lateral stress ratio plotted against axial effective stress from the K_0 compression test on sample T2 (III).

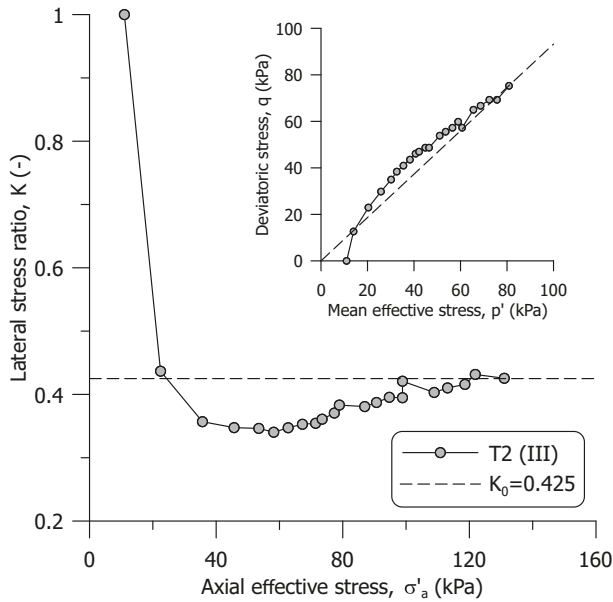
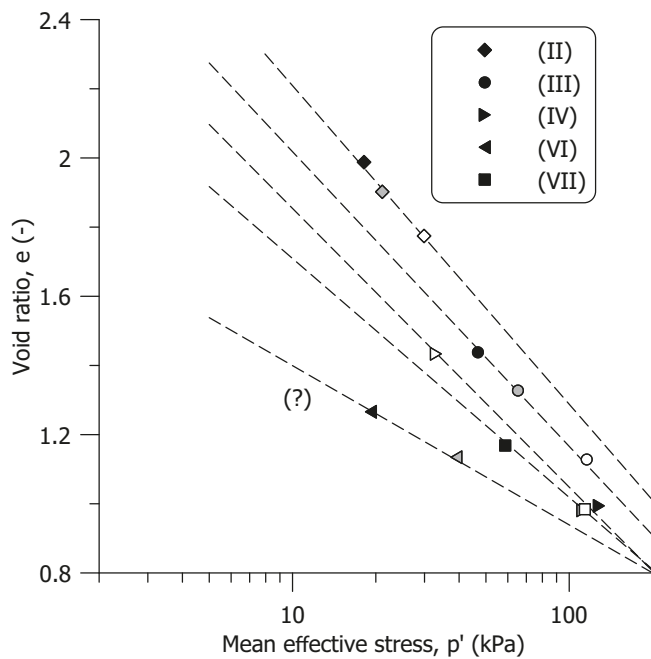


Fig. 9. Ultimate state in the $e-p'$ attained by samples from different groups after shearing.



from 0.040 to 0.017. The dependence of the compression response on the LOI found in Fig. 10 aligns well with a large dataset of experimental results from oedometer tests on Bogotá clay samples encompassing a wide range of loss on ignition, displayed in Fig. 11 (redrawn from Reina Leal 2019).

Numerous correlations between the compression coefficient and index properties (e.g., liquid limit) have been proposed in the literature for fine-grained materials (Balasubramaniam and Brenner 1981). Among the proposals, the experimental data are compared in Fig. 12a with the

relationship proposed by Skempton and Jones (1944) for remoulded clays and Terzaghi and Peck (1967) for normally consolidated clays. The comparison shows that the tested material exhibits higher compressibility than that predicted by empirical correlations on inorganic soils. The experimental data align well with the correlation proposed by Caicedo et al. (2018) for Bogotá organic clays.

Noteworthy, the increase in the compressibility of the tested material is not associated with an increasing percentage of clay fraction as commonly found for inorganic soils (Skempton and Jones 1944). On the contrary, the compressibility is found to decrease with the clay fraction as displayed in Fig. 12b. The evidence is explained by the influence of the organic matter and diatoms on the soil compressibility, as already noticed by Caicedo et al. (2018). Although both the LOI and the clay content contribute to the liquid limit, the former predominates in the investigated material, as the positive correlation in Fig. 10 demonstrates. This correlation allows inferring the compressibility of the tested soil from both:

$$(3) \quad C_c = 0.01w_l$$

and

$$(4) \quad C_c = 0.07 + 0.11LOI$$

where w_l and LOI are expressed in percentages. Equation 4 is particularly useful in those countries where organic soils are abundant, and the LOI determination is included in the standard practice classification procedure, more than Atterberg limits.

The ratio λ/κ over different values of LOI is reported in Fig. 13. The results show a slight tendency for the λ/κ ratio to decrease with the organic matter, approaching a fairly constant value of 9 at increasing LOI. A lower value for the λ/κ ratio of 7.6 is reported by Caicedo et al. (2018) for diatomaceous soil in lacustrine deposits of Bogotá with an LOI ranging from 2% to 20%.

The variation in the compression index shown in Fig. 10 has been attributed primarily to the presence of organic matter. It is worth noting that different diatoms content could also contribute to the observed response. However, if the observed differences in compressibility were only due to a higher diatoms content, differences in the shearing response among the different samples would also be expected. Shiwakoti et al. (2002) tested artificial mixtures of Singapore clay and diatoms. For a diatom content increasing from 0% to 40%, a 1.9-fold increase in the compression index, C_c , was observed, similar to the one in Fig. 10a. However, the increase in diatom content also led to a 10° increase in the ultimate friction angle, which was not observed in our study (Fig. 9). The evidence suggests that the difference in compressibility for the tested material could be attributed primarily to variations in the microorganisms-related organic matter. Similar composition and fabric, including highly decomposed wood fragments, microorganisms, and amorphous organic, were found in the Oostvaardersplassen clay by Cheng et al. (2004, 2007). The absence of significant differences in the ultimate friction angle within the investigated loss on ignition also suggests that the decomposed plant fibres do not have a significant reinforcing effect contrary to what is observed in

Fig. 10. Dependence of the slope of the compression line (a) and unloading-reloading line (b) on the loss on ignition for different loading directions.

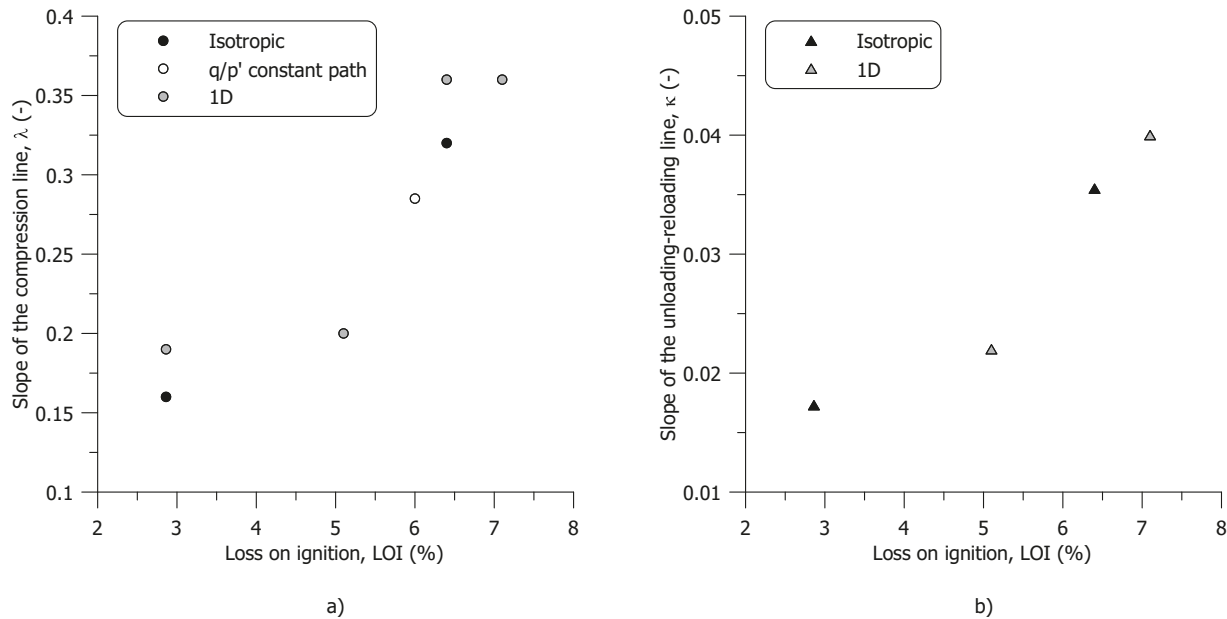
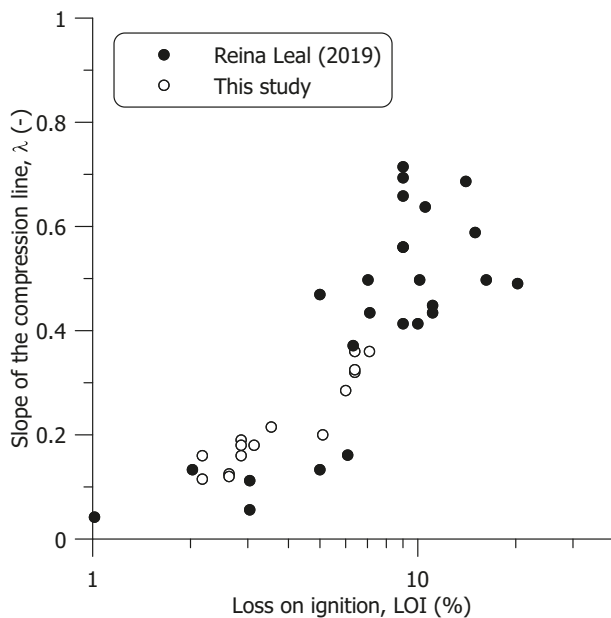


Fig. 11. Variation of the slope of the compression line with the loss on ignition (redrawn from Reina Leal 2019).



fibrous soils. The organic matter of this type is hardly visible in ESEM, although it was discovered by Tribovillard et al. (2022) inside pyrite framboids similar to the ones in Fig. 3c.

To broaden the view of the compression behaviour, the dependence of the compressibility on the loading direction is investigated. To this aim, results on the volumetric response of samples from group (III) are analysed including isotropic, K_0 compression, and a stress path at a constant stress ratio $q/p' = 0.2$. The slope of the compression line for each loading

direction and of the critical state line normalised with the one along isotropic loading (λ/λ_{iso}) are compared in Fig. 14.

The results show a dependence of the slope of the compression line on the loading direction, with λ increasing with the stress ratio. Similar evidence of the dependence of the slope of the normal compression line on the stress path direction was also found by Rampello et al. (1997) on reconstituted samples of Vallericca clay.

Coupled deviatoric-volumetric deformation behaviour

The pre-failure plastic deformation behaviour is analysed in terms of plastic strain increment vectors. The post-yielding portions of the constant q/p' paths from groups (III) and (VII) (Fig. 4) are considered. The inclination of the plastic strain increment vectors, β , defined in eq. 5 is plotted as a function of the mean effective stress in Fig. 15 for each test.

$$(5) \quad \tan \beta = \frac{\delta \epsilon_q^p}{\delta \epsilon_p^p}$$

The volumetric and the deviatoric plastic strain increments, $\delta \epsilon_p^p$ and $\delta \epsilon_q^p$, have been derived from the total ones by computing the elastic strains with a hypo-elastic isotropic law assuming a constant Poisson's ratio, $\nu = 0.2$. For each path, the value of κ has been either determined from the experimental data in Fig. 10, when available, or computed from the polynomial interpolation in Fig. 14, assuming an average $\lambda/\kappa = 9.1$.

The results in Fig. 15b show an anisotropic plastic deformation behaviour. The plastic strain increment vectors show a progressive rotation along the stress paths. The magnitude of the rotation seems to depend on the previous stress history and the loading direction, as first suggested by Lewin and Burland (1970) and Lewin (1973) in a study dedicated to

Fig. 12. Correlation of the compression coefficient with the liquid limit (a) and (b) the clay fraction.

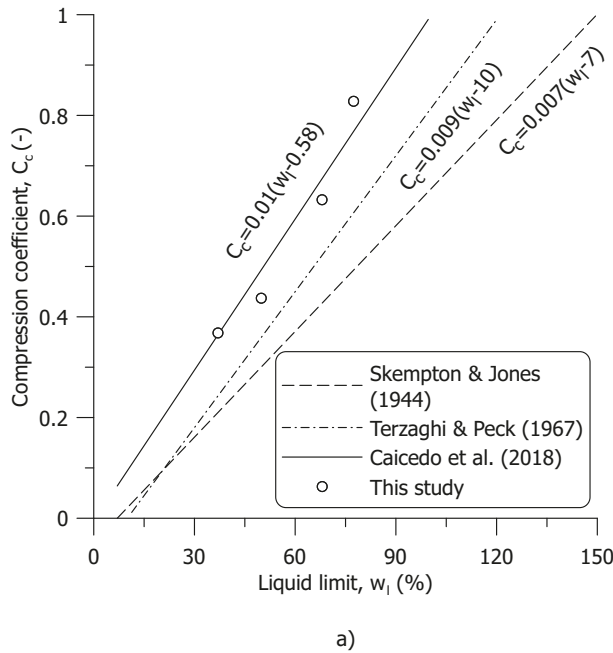


Fig. 13. Influence of the loss on ignition on the ratio between the slope of the compression line and the unloading-reloading line.

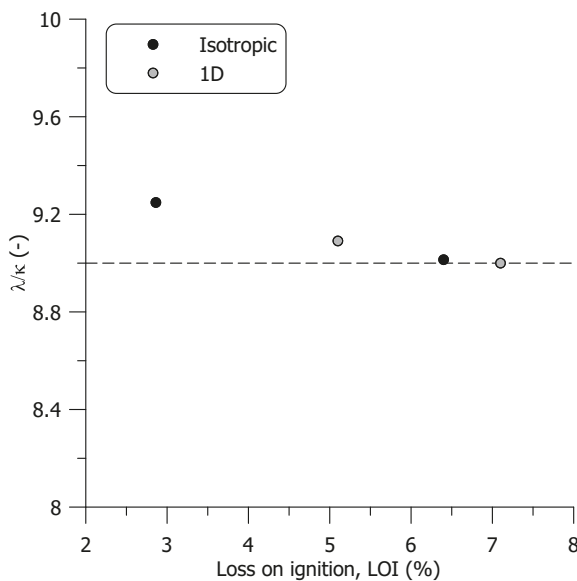
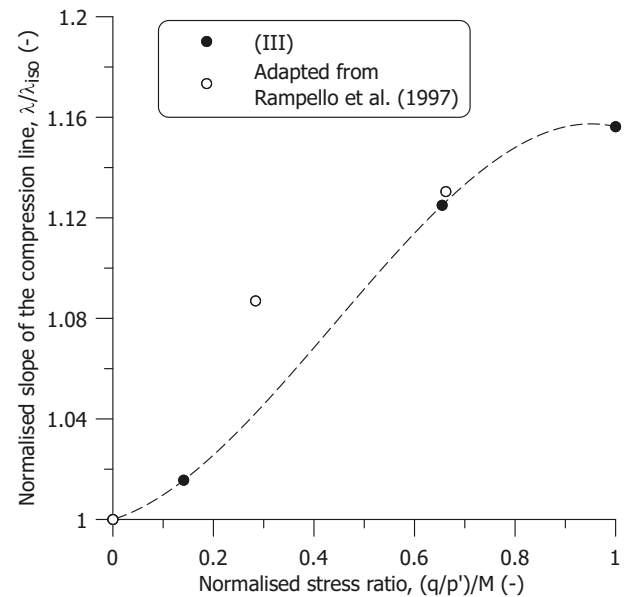


Fig. 14. Dependence of the slope of the compression line on the loading direction.



the flow rule of clays. For the K_0 compression tests on samples T2 (III) and T2 (VII), the plastic strain increment vectors do not rotate as a result of the initial alignment of the fabric along the K_0 line. On the contrary, along the subsequent path $q/p' = 0.48$, the plastic strain increment vectors realign as a result of the difference between the current stress path and the previous stress history of the sample (sample T2 (III) Fig. 15a). For sample T3 (III), along the path $q/p' = 0.2$, the rotation is very limited due to the previous isotropic consoli-

dation up to $p'_c = 67$ kPa (Table 1), which realigned the plastic strain increment vectors along the p' -axis. The magnitude of the rotation increases in the next paths along $q/p' = 0.48$ and $q/p' = 0.98$.

If the plastic strain increment vectors in Fig. 15b are assumed to have reached the final inclination for each constant q/p' stress path (i.e., saturation condition), they can be used to derive information on the stress-dilatancy relationship. Figure 16 presents the dilatancy, $d = 1/\tan\beta$, derived

Fig. 15. Stress paths (a) and (b) evolution of the inclination of the plastic strain increment vectors.

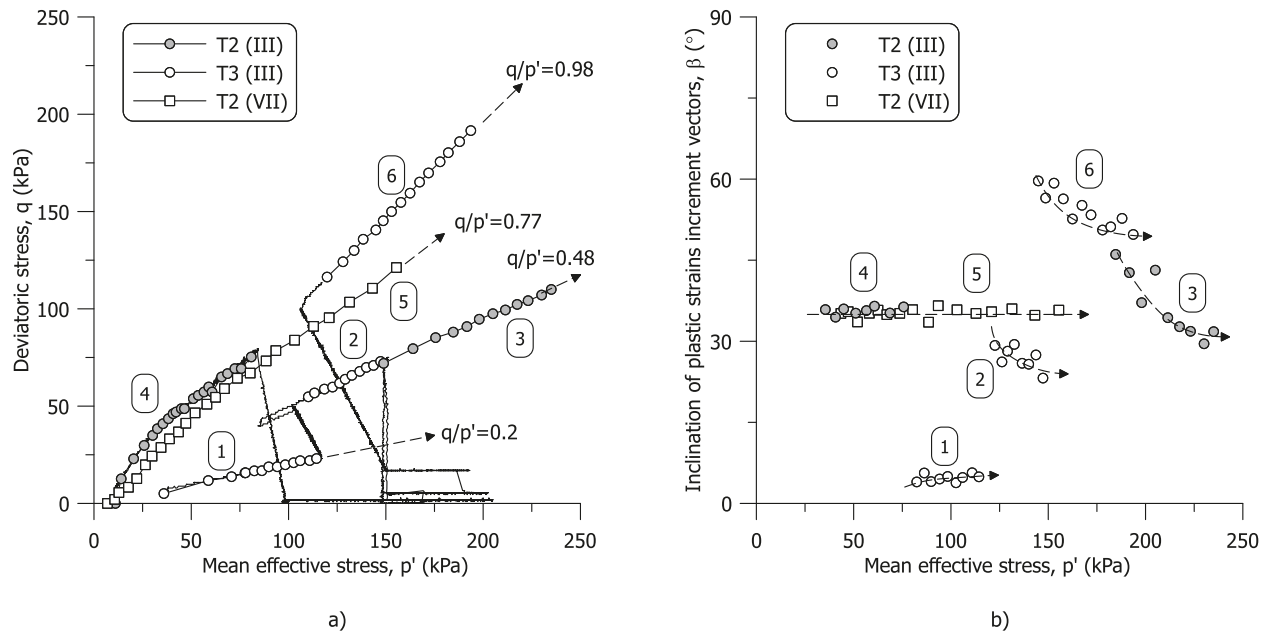
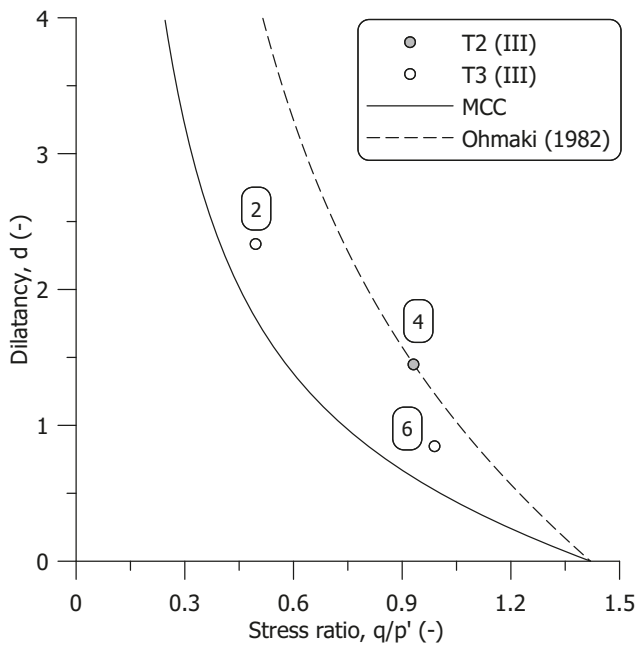


Fig. 16. Comparison between dilatancy from experimental results and common isotropic stress-dilatancy relationships.



from experimental data of group (III), compared with common isotropic stress-dilatancy relationships.

The comparison with the K_0 compression test (point 4 in Fig. 16) confirms the well-known limitation of the Modified Cam clay model, MCC (Roscoe and Burland 1968), which tends to overestimate the K_0 value (Gens and Potts 1982; Alonso et al. 1990). To avoid this shortcoming, the expression of the stress-dilatancy relationship of the MCC is often modified by means of a shape parameter χ_g resulting in

(Ohmaki 1982):

$$(6) \quad d = \frac{M^2 - \eta^2}{\chi_g \eta}$$

with $\eta = q/p'$. For $\chi_g = 2$, the stress-dilatancy relationship of the MCC is recovered. The shape coefficient in eq. 6, $\chi_g = 0.85$, is calibrated on the K_0 compression test. As shown in Fig. 16, despite the calibration of χ_g to match the K_0 path, the experimental dilatancy for the other constant q/p' stress paths does not align with the new relationship. The experimental evidence suggests that the plastic deformation mechanism changes with the loading direction and that the stress-dilatancy relationship cannot be formulated as a unique function of the stress ratio, $d = d(\eta)$.

Conclusions

The laboratory characterisation of an organic silty-clay from the Netherlands is presented in this study. The material exhibits naturally varying organic content, with loss on ignition decreasing from 7% to 3% with depth. The fabric is organised into aggregates with a characteristic size of 50–100 μm in which silty particles, diatom inclusions, and small wood fragments are visible. Comparison between the particle size distribution across the samples suggests that the organic matter is mainly included in the silty fraction.

Oedometer and triaxial compression tests indicate a dependence of the compressibility on the organic matter. The slope of the compression line, λ , and unloading reloading line, κ , decreases from 0.360–0.160 and from 0.040–0.017, respectively, across the range of loss on ignition investigated. The compressibility data also align with the relationship proposed by Caicedo et al. (2018) giving the compression coefficient as a function of the liquid limit. The λ/κ ratio slightly decreases at increasing organic matter and levels off at a relatively constant value of 9.

Compression tests along stress paths at constant stress ratio show a dependence of the slope of the compression line on the loading direction, with λ increasing with the stress ratio. Anisotropic post-yielding behaviour is observed where plastic strain increment vectors realign over stress paths at a constant stress ratio. The magnitude of this realignment depends on the previous stress history and the loading direction. The experimental evidence suggests that the stress–dilatancy relationship of this material cannot be formulated as a single function of the stress ratio.

All the samples attain a similar ultimate stress ratio corresponding to a friction angle in triaxial compression of 35° regardless of the loss on ignition. This suggests that the effects of the organic matter on shear strength are less significant than on compression. However, the data show that a critical state line can only be identified for samples with similar organic content. A general trend is observed, with the intercept and slope of the critical state line increasing with the organic matter. The active K_0 compression test in the triaxial apparatus shows that the critical state friction angle and the at-rest lateral earth pressure coefficient in normally consolidated conditions are well related by Jaky's simplified relationship. The response upon compression and the absence of significant post-failure brittleness during shear seem to indicate that destructuration does not occur within the investigated stress range.

The high-quality data presented in this study enrich the available database on soft silty-clays of marine origin containing non-fibrous organic matter and a moderate amount of diatoms. The data provide few hints on the advanced modelling of the volumetric and deviatoric pre-failure behaviour of these soils.

List of symbols

G_s	specific gravity
LOI	loss on ignition
e	void ratio
e_i	initial void ratio
ε_a	axial strain
ε_r	radial strain
ε_p	volumetric strain
ε_q	deviatoric strain
ν	Poisson's ratio
H_0	initial sample height
V_0	initial sample volume
H	current sample height
V	current sample volume
w_p	plastic limit
w_l	liquid limit
I_p	plasticity index
C_c	compression coefficient
C_s	unloading-reloading coefficient
λ	slope of the compression line
λ_{iso}	slope of the isotropic compression line
κ	slope of the unloading-reloading line
OCR	overconsolidation ratio
σ'_v	vertical effective stress
σ'_a	axial effective stress

p'	mean effective stress
q	deviatoric stress
K	lateral stress ratio
K_0	coefficient of earth pressure at rest
η	stress ratio
M	ultimate stress ratio
ϕ'	friction angle
p'_c	pre-consolidation mean effective stress
p'_s	mean effective stress at the start of the shear
Γ	intercept of the critical state line
d	dilatancy
χ_g	shape parameter for the stress–dilatancy relationship
$\delta\varepsilon_p^p$	volumetric plastic strain increment
$\delta\varepsilon_q^p$	deviatoric plastic strain increment
β	inclination of the plastic strain increment vectors
q_t	corrected cone resistance
f_s	sleeve friction

Acknowledgement

The financial support of the Dutch Organisation for Scientific Research (NWO), under the project “Reliability-Based Geomechanical Assessment Tools for Dykes and Embankments in Delta Areas - 13864 (Reliable Dykes)”, is gratefully acknowledged.

Article information

History dates

Received: 6 February 2023

Accepted: 16 November 2023

Accepted manuscript online: 29 November 2023

Version of record online: 6 June 2024

Copyright

© 2024 The Author(s). Permission for reuse (free in most cases) can be obtained from [copyright.com](https://creativecommons.org/licenses/by/4.0/).

Data availability

Data generated or analysed during this study are available from the corresponding author upon motivated request.

Author information

Author ORCIDs

Stefano Muraro <https://orcid.org/0000-0003-0737-9378>

Cristina Jommi <https://orcid.org/0000-0002-9439-528X>

Author notes

Cristina Jommi served as Editorial Board Member at the time of manuscript review and acceptance and did not handle peer review and editorial decisions regarding this manuscript.

Author contributions

Conceptualization: SM

Data curation: EP

Investigation: EP

Methodology: EP

Supervision: AN, CJ

Visualization: SM

Writing – original draft: SM

Writing – review & editing: AN, CJ

Competing interests

The authors declare there are no competing interests.

References

- Alonso, E.E., Gens, A., and Josa, A. 1990. A constitutive model for partially saturated soils. *Géotechnique*, **40**(3): 405–430. doi:[10.1680/geot.1990.40.3.405](https://doi.org/10.1680/geot.1990.40.3.405).
- Balasubramaniam, A.S., and Brenner, R.P. 1981. Consolidation and settlement of soft clay. In *Soft clay engineering*. Edited by E.W. Brand and R.P. Brenner, Elsevier, Amsterdam. pp. 481–566.
- BS1377. 1996. Methods of test for soils for civil engineering purposes Part 2. Classification tests. British Standard Institution, London.
- Burland, J.B. 1990. On the compressibility and shear strength of natural clays. *Géotechnique*, **40**(3): 329–378. doi:[10.1680/geot.1990.40.3.329](https://doi.org/10.1680/geot.1990.40.3.329).
- Caicedo, B., Mendoza, C., López, F., and Lizcano, A. 2018. Behavior of diatomaceous soil in lacustrine deposits of Bogotá, Colombia. *Journal of Rock Mechanics and Geotechnical Engineering*, **10**(2): 367–379. doi:[10.1016/j.jrmge.2017.10.005](https://doi.org/10.1016/j.jrmge.2017.10.005).
- Cheng, X.H., Janssen, H., Barends, F.B.J., and Den Haan, E.J. 2004. A combination of ESEM, EDX and XRD studies on the fabric of Dutch organic clay from Oostvaardersplassen (Netherlands) and its geotechnical implications. *Applied Clay Science*, **25**(3–4): 179–185. doi:[10.1016/j.clay.2003.11.002](https://doi.org/10.1016/j.clay.2003.11.002).
- Cheng, X.H., Ngan-Tillard, D.J.M., and Den Haan, E.J. 2007. The causes of the high friction angle of Dutch organic soils. *Engineering Geology*, **93**(1): 31–44. doi:[10.1016/j.enggeo.2007.03.009](https://doi.org/10.1016/j.enggeo.2007.03.009).
- D2974-14, A. 2014. Standard test methods for moisture, ash, and organic matter of peat and other organic soils. American Society of Testing and Materials.
- D5550-14, A. 2014. Standard test method for specific gravity of soil solids by gas pycnometer. American Society of Testing and Materials, West Conshohocken, PA, USA.
- de Bakker, H. 1979. Major soils and soil regions in the Netherlands. W. Junk, B.V. Publishers, The Hague, the Netherlands.
- Den Haan, E.J. 2003. Sample disturbance of soft organic Oostvaardersplassen clay. Deformation characteristics of geomaterials. Edited by H. Di Benedetto, T. Doanh, H. Geoffroy and C. Sauzéat. A.A. Balkema, Lisse, The Netherlands, pp. 49–55.
- Den Haan, E.J., and Kruse, G.A.M. 2007. Characterisation and engineering properties of Dutch peats. In *Proceedings of the Second International Workshop of Characterisation and Engineering Properties of Natural Soils*. Singapore 2007. Edited by T.S. Tan, K.K. Phoon, D.W. Hight and S. Leroueil. CRC Press (Taylor & Francis Group), Boca Raton, FL, USA, pp. 2101–2133.
- Diaz-Rodriguez, J.A., Leroueil, S., and Aleman, J.D. 1992. Yielding of Mexico City clay and other natural clays. *Journal of Geotechnical Engineering*, **118**(7): 981–995. doi:[10.1061/\(ASCE\)0733-9410\(1992\)118:7\(981\)](https://doi.org/10.1061/(ASCE)0733-9410(1992)118:7(981)).
- Gens, A., and Potts, D.M. 1982. A theoretical model for describing the behaviour of soils not obeying Rendulic's principle. In *Proceedings of the International Symposium on Numerical Models in Geomechanics*, Zurich, Switzerland. pp. 24–32.
- Head, K.H. 2014. Manual of soil laboratory testing—vol. I: soil classification and compaction tests. Whitteles Publishing, Dunbeath, UK.
- Hendry, M.T., Martin, C.D., and Barbour, S. 2013. Measurement of cyclic response of railway embankments and underlying soft peat foundations to heavy axle loads. *Canadian Geotechnical Journal*, **50**(5): 467–480. doi:[10.1139/cgj-2012-0118](https://doi.org/10.1139/cgj-2012-0118).
- Hight, D.W., Bond, A.J., and Legge, J.D. 1992. Characterization of the Bothkennar clay: an overview. *Géotechnique*, **42**(2): 303–347. doi:[10.1680/geot.1992.42.2.303](https://doi.org/10.1680/geot.1992.42.2.303).
- Jommi, C., Chao, C.Y., Muraro, S., and Zhao, H.F. 2021. Developing a constitutive approach for peats from laboratory data. *Geomechanics for Energy and the Environment*, **27**: 100220. doi:[10.1016/j.gete.2020.100220](https://doi.org/10.1016/j.gete.2020.100220).
- Larsson, R. 1990. Behaviour of organic clay and gyttja. Swedish Geotechnical Institute, Linköping.
- Lewin, P.I. The influence of stress history on the plastic potential. In *Proceedings of the Symposium on the Role of Plasticity in Soil Mechanics*, Cambridge, England. pp. 96–105.
- Lewin, P.I., and Burland, J.B. 1970. Stress-probe experiments on saturated normally consolidated clay. *Géotechnique*, **20**(1): 38–56. doi:[10.1680/geot.1970.20.1.38](https://doi.org/10.1680/geot.1970.20.1.38).
- Lo, K.Y. 1962. Shear strength properties of a sample of volcanic material of the Valley of Mexico. *Géotechnique*, **12**(4): 303–318. doi:[10.1680/geot.1962.12.4.303](https://doi.org/10.1680/geot.1962.12.4.303).
- Ludwik, P. 1909. *Elemente der technologischen Mechanik*. Springer-Verlag, Berlin, Germany.
- Mesri, G., Rokhsar, A., and Bohor, B.F. 1975. Composition and compressibility of typical samples of Mexico City clay. *Géotechnique*, **25**(3): 527–554. doi:[10.1680/geot.1975.25.3.527](https://doi.org/10.1680/geot.1975.25.3.527).
- Muraro, S. 2019. The deviatoric behaviour of peat: a route between past empiricism and future perspectives. PhD thesis, Delft University of Technology, Delft, the Netherlands.
- Muraro, S., and Jommi, C. 2021. Experimental determination of shear strength of peat from standard undrained triaxial tests: correcting for the effects of end restraint. *Géotechnique*, **71**(1): 76–87. doi:[10.1680/jgeot.18.P.346](https://doi.org/10.1680/jgeot.18.P.346).
- Ohmaki, S. 1982. Stress-strain behaviour of anisotropically, normally consolidated cohesive soil. In *Proceeding 1st International Symposium on Numerical Models in Geomechanics*. Zurich, Switzerland. pp. 250–269.
- Paul, M.A., and Barras, B.F. 1999. Role of organic material in the plasticity of Bothkennar clay. *Géotechnique*, **49**(4): 529–535. doi:[10.1680/geot.1999.49.4.529](https://doi.org/10.1680/geot.1999.49.4.529).
- Ponzoni, E. 2017. Historical constructions on natural silty soils accounting for the interaction with the atmosphere. PhD thesis, Università degli studi di Brescia, Brescia, Italy.
- Rampello, S., Viggiani, G.M.B., and Amorosi, A. 1997. Small-strain stiffness of reconstituted clay compressed along constant triaxial effective stress ratio paths. *Géotechnique*, **47**(3): 475–489. doi:[10.1680/geot.1997.47.3.475](https://doi.org/10.1680/geot.1997.47.3.475).
- Reina Leal, R.C. 2019. Influencia del contenido de Materia Orgánica en el cambio volumétrico de arcillas blandas. MSc thesis, Universidad Nacional de Colombia, Bogotá, Colombia.
- Roscoe, K.H., and Burland, J.B. 1968. On the generalized stress-strain behaviour of wet clay. In *Engineering plasticity*. Edited by J. Heyman and F.A. Leckie. Cambridge University Press, Cambridge, pp. 535–609.
- Shiwakoti, D.R., Tanaka, H., Tanaka, M., and Locat, J. 2002. Influences of diatom microfossils on engineering properties of soils. *Soils and Foundations*, **42**(3): 1–17. doi:[10.3208/sandf.42.3_1](https://doi.org/10.3208/sandf.42.3_1).
- Skempton, A.W., and Jones, O.T. 1944. Notes on the compressibility of clays. *QJGS*, **100**(1–4): 119–135. doi:[10.1144/GSL.JGS.1944.100.01-04.08](https://doi.org/10.1144/GSL.JGS.1944.100.01-04.08).
- Tanaka, H., and Locat, J. 1999. A microstructural investigation of Osaka Bay clay: the impact of microfossils on its mechanical behaviour. *Canadian Geotechnical Journal*, **36**(3): 493–508. doi:[10.1139/t99-009](https://doi.org/10.1139/t99-009).
- Terzaghi, K., and Peck, R.B. 1967. *Soil mechanics in engineering practice*. Wiley, New York.
- Tigheelaar, J., De Feijter, J.W., and Den Haan, E.J. 2001. Shear tests on reconstituted Oostvaardersplassen clay. In *Soft Ground Technology*. ASCE (American Society of Civil Engineers), Reston, VA, pp. 67–81.
- Tribouillard, N., Bout-Roumazielles, V., Delattre, M., Ventalon, S., and Bensadok, A. 2022. Sedimentary pyrite as a trap of organic matter: preliminary results from large-framboid observation. *European Journal of Mineralogy*, **34**(1): 77–83. doi:[10.5194/ejm-34-77-2022](https://doi.org/10.5194/ejm-34-77-2022).
- Watabe, Y., Tanaka, M., Tanaka, H., and Tsuchida, T. 2003. K₀ consolidation in a triaxial cell and evaluation of in-situ K₀ for marine clays with various characteristics. *Soils and Foundations*, **43**(1): 1–20. doi:[10.3208/sandf.43.1](https://doi.org/10.3208/sandf.43.1).
- Zwanenburg, C., and Jardine, R.J. 2015. Laboratory, in situ and full-scale load tests to assess flood embankment stability on peat. *Géotechnique*, **65**(4): 309–326. doi:[10.1680/geot.14.P.257](https://doi.org/10.1680/geot.14.P.257).
- Zwanenburg, C., Den Haan, E.J., Kruse, G.A.M., and Koelewijn, A.R. 2012. Failure of a trial embankment on peat in Booneschans, the Netherlands. *Géotechnique*, **62**(6): 479–490. doi:[10.1680/geot.9.P.094](https://doi.org/10.1680/geot.9.P.094).